2012

Effects of selective bile duct ligation on liver parenchyma in young animals: histologic and molecular evaluations

JOURNAL OF PEDIATRIC SURGERY, PHILADELPHIA, v. 47, n. 3, supl. 1, Part 4, pp. 513-522, MAR, 2012

http://www.producao.usp.br/handle/BDPI/34209

Journal of Pediatric Surgery (2012) 47, 513–522

ELSEVIER

Journal of Pediatric Surgery

www.elsevier.com/locate/jpedsurg

Effects of selective bile duct ligation on liver parenchyma in young animals: histologic and molecular evaluations☆

Ana Cristina A. Tannuri, Maria Cecília M. Coelho, Josiane de Oliveira Gonçalves, Maria Mercês Santos, Luiz Fernando Ferraz da Silva, Israel Bendit, Uenis Tannuri*

Pediatric Surgery Division, Pediatric Liver Transplantation Unit and Laboratory of Research in Pediatric Surgery (LIM 30), University of Sao Paulo Medical School; Sao Paulo, Brazil

Received 13 May 2011; revised 7 September 2011; accepted 7 October 2011

Key words:
Cholestasis;
Models animal;
Biliary atresia;
Liver transplantation;
Actins;
Transforming growth factor β1;
Desmin;
Reverse transcriptase–polymerase chain reaction

Abstract

Background/Purpose: The mechanisms of increased collagen production and liver parenchyma fibrosis are poorly understood. These phenomena are observed mainly in children with biliary obstruction (BO), and in a great number of patients, the evolution to biliary cirrhosis and hepatic failure leads to the need for liver transplantation before adolescence. However, pediatric liver transplantation presents with biliary complications in 20% to 30% of cases in the postoperative period. Intra- or extrahepatic stenosis of bile ducts is frequent and may lead to secondary biliary cirrhosis and the need for retransplantation. It is unknown whether biliary stenosis involving isolated segments or lobes may affect the adjacent nonobstructed lobes by paracrine or endocrine means, leading to fibrosis in this parenchyma. Therefore, the present study aimed to create an experimental model of selective biliary duct ligation in young animals with a subsequent evaluation of the histologic and molecular alterations in liver parenchyma of the obstructed and nonobstructed lobes.

Methods: After a pilot study to standardize the surgical procedures, weaning rats underwent ligation of the bile ducts of the median, left lateral, and caudate liver lobes. The bile duct of the right lateral lobe was kept intact. To avoid intrahepatic biliary duct collaterals neoformation, the parenchymal connection between the right lateral and median lobes was clamped. The animals were divided into groups according to the time of death: 1, 2, 3, 4, and 8 weeks after surgical procedure. After death, the median and left lateral lobes (with BO) and the right lateral lobe (without BO [NBO]) were harvested separately. A group of 8 healthy nonoperated on animals served as controls. Liver tissues were subjected to histologic evaluation and quantification of the ductular proliferation and of the portal fibrosis. The expressions of smooth muscle α-actin (α-SMA), desmin, and transforming growth factor β1 genes were studied by molecular analyses (semiquantitative reverse transcriptase–polymerase chain reaction and real-time polymerase chain reaction, a quantitative method).

Results: Histologic analyses revealed the occurrence of ductular proliferation and collagen formation in the portal spaces of both BO and NBO lobes. These phenomena were observed later in NBO than BO. Bile duct density significantly increased 1 week after duct ligation; it decreased after 2 and 3 weeks and then increased again after 4 and 8 weeks in both BO and NBO lobes. The portal space collagen area

☆ Grants from CNPQ number 478407/2008-4.

* Corresponding author. Faculdade de Medicina da Universidade de São Paulo, São Paulo–SP, CEP: 01246-903, Brazil. Tel.: +55 11 30812943; fax: +55 11 32556285.

E-mail address: uenist@usp.br (U. Tannuri).

doi:10.1016/j.jpedsurg.2011.10.009

increased after 2 weeks in both BO and NBO lobes. After 3 weeks, collagen deposition in BO was even higher, and in NBO, the collagen area started decreasing after 2 weeks. Molecular analyses revealed increased expression of the α-SMA gene in both BO and NBO lobes. The semiquantitative and quantitative methods showed concordant results.

Conclusions: The ligation of a duct responsible for biliary drainage of the liver lobe promoted alterations in the parenchyma and in the adjacent nonobstructed parenchyma by paracrine and/or endocrine means. This was supported by histologic findings and increased expression of α-SMA, a protein related to hepatic fibrogenesis.

The mechanisms of increased collagen production and liver parenchyma fibrosis are poorly understood [1,2]. These phenomena are particularly observed in children with biliary obstruction (BO) in whom the evolution to biliary cirrhosis and hepatic failure leads to the need for liver transplantation.

However, pediatric liver transplantation presents with biliary complications in 20% to 30% of cases in the postoperative period [3]. Intra- or extrahepatic stenosis of bile ducts are frequent and may lead to secondary biliary cirrhosis and the need for retransplantation [3]. It is unknown whether biliary stenosis involving isolated segments or lobes may affect the adjacent nonobstructed lobes by paracrine or endocrine means, leading to fibrosis in this parenchyma.

During liver fibrogenesis, stellate cells (Ito cells) are activated and transformed into myofibroblasts [4]. There is evidence that stellate cells in rats express desmin, and when activated, they also express smooth muscle α-actin (α-SMA) [5]. Desmin and α-SMA are structural proteins of the intermediary filaments that are present in the cytoskeleton of smooth muscle cells and other cell types. These cells are then responsible for the increased synthesis of type I collagen. Another important profibrogenic cytokine implicated in this process is transforming growth factor β1 (TGF-β1) [6]. Type I collagen gene expression in Ito cells is regulated at the transcriptional level by TGF-β1 [7].

Although much is known about cell injury and fibrosis induction because of liver diseases, some aspects remain unclear, such as the nature of the differences between the diseases seen in newborn infants and those in older children and adults [8]. The classic experimental model used to study of BO is the common bile duct ligation in rats [5,9,10]. However, the response of young animals to bile duct ligation has yet to be completely understood. In addition, there is no experimental model of selective bile duct ligation in young animals that simulates the condition of isolated bile duct stenosis commonly observed in the postoperative period of a liver-transplanted child.

Based on these shortcomings, the present study aimed to create an experimental model of selective biliary duct ligation in young animals, with a subsequent evaluation of the histologic and molecular alterations in liver parenchyma of the obstructed and nonobstructed lobes.

1. Methods

1.1. Animals

Fifty-nine weaning Wistar rats (age, 21-23 days; weight, 30-50 g) were used. All animals received care according to the criteria outlined in the Guide for the Care and Use of Laboratory Animals prepared by the National Academy of Sciences [11]. This study protocol was reviewed and approved by the animal ethics committee of our institution (University of São Paulo Medical School, São Paulo, Brazil).

The weaning rats were maintained on standard laboratory diet and tap water ad libitum throughout the experiment.

1.2. Surgical procedures

All animals were operated on by the same surgeon (ACAT). The surgical procedures were performed under sterile conditions using ether anesthesia.

Using surgical microscope (original magnification ×20) and microsurgical instruments, a midline incision (2 cm in length) was made in the upper abdomen. A double ligation with 9-0 prolene and section of the bile ducts of the median, left lateral, and caudate liver lobes was performed. The bile duct of the right lateral lobe was kept intact (Fig. 1).

To avoid intrahepatic biliary duct collaterals neoformation, the parenchyma connection between the right lateral and median lobes was clamped with the aid of a hemostatic clip. After this procedure, it was verified that the right lateral lobe was completely isolated from the rest of the hepatic parenchyma (Fig. 1). The abdomen was closed with a continuous suture, in a single layer, with 6-0 prolene. After surgery, the animals were given a regular diets and water ad libitum. A group of 8 healthy nonoperated on animals served as a control.

The rats were killed 1, 2, 3, 4, or 8 weeks after the operation (8 animals per group) under ether anesthesia, and the body weights were then measured. A midline abdominal and thoracic incision was performed to harvest liver lobes. The median and left lateral lobes (with BO) and the right lateral lobe (without BO [NBO]) were harvested separately. Liver tissues were fixed in 10% neutral-buffered formalin for histologic examination and quantification of the ductular proliferation

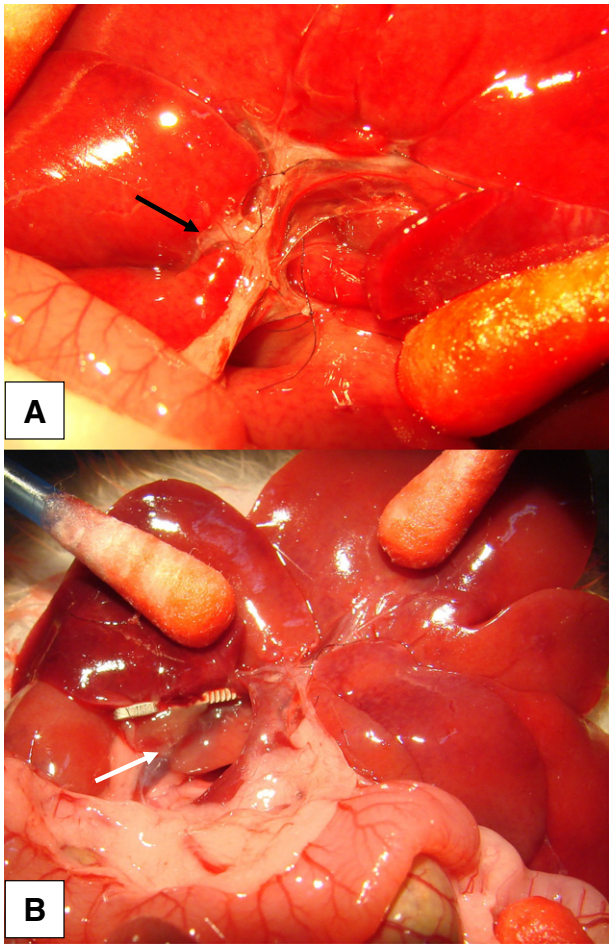

Fig. 1 A, Photograph showing the ligation and section of the median, left lateral, and caudate liver lobe ducts. Note that the bile duct of the right lateral lobe is kept intact (black arrow). B, The parenchymal connection between the right lateral and median lobes is clamped with a hemostatic clip (white arrow).

and of the portal fibrosis. The liver tissue obtained from animals killed 1 week after selective biliary ligation was, in addition, snap frozen in liquid nitrogen at −170°C for subsequent molecular analyses. The expressions of α-SMA, desmin, and TGF-β1 genes were studied by reverse transcriptase–polymerase chain reaction (RT-PCR), a semiquantitative method, and the altered gene expression was checked by real-time polymerase chain reaction (PCR), a quantitative method.

1.3. Histologic examinations

The fragments of liver biopsies were kept in a buffer solution with 10% formaldehyde for a period of 24 to 48 hours, and then, they were embedded in paraffin. Three-micrometer-thick histologic cuts from the paraffin blocks were obtained from all groups of animals and were subjected to hematoxylin-eosin (HE) and picrosirius staining. The slides were analyzed in a Nikon binocular microscope and photographed with a Nikon FX DS-Fi1 camera (Nikon Corporation, Tokyo, Japan).

In HE-stained slides, general liver morphology and histologic alterations caused by biliary duct ligation were evaluated qualitatively by 2 blinded pathologists.

1.3.1. Quantification of ductular proliferation and portal fibrosis

The ductular proliferation and portal fibrosis at several phases of the experiment were studied by the Sirius red staining technique [12]. The quantification of collagen was performed using the Kontron Electronic 300 Image Analysis System (Zeiss, Munich, Germany). The workstation consisted of a Nikon bifocal light microscope, a colored videocamera, a digitizing board for image capture, and a Pentium microcomputer with a 133 MHz processor (Hewlett Packard, Palo Alto, CA) operating on a Windows XP platform (Microsoft Corporation, Redmond, WA). The images were digitized with the aid of specific software (NIS Elements BR, Nikon Corporation, Tokyo, Japan), allowing data sharing with the word processor (Microsoft Word) and spreadsheet (Microsoft Excel). The optical transmission was calibrated and quantified to process and analyze the image, so it could be quantified on the monitor according to its original measurements. To obtain data as absolute values, a 1-mm calibration slide with 100 divisions (Nikon) was used, and each division corresponded to 10 μm. Image calibration was performed for images obtained at 10×, 20×, 40×, and 100×. This quantification was performed at the smallest spatial unit, called a *pixel*. The calibration factor was automatically calculated in pixels and used by the program for the corresponding calculations in micrometers according to the calibration. The images were analyzed by the Image Pro Plus program (Media Cybernetics, Inc, Bethesda, MD) using its resources for determining area, volume, length, and particle counting. This tool allowed the identification of a certain structure, its labeling, and automatization of its identification for future readings as well as allowing the use of filters and the use of macros for the automatization of several tasks.

The histologic cuts were processed in the image analysis system using an objective lens ×20 and an ocular lens ×10. The images were captured by the videocamera and processed in special boards for computer image digitization to optimize the results. After obtaining the images, the portal space areas to be measured were delineated with the help of a computer mouse. Biliary ducts inside this portal space were counted. A graphic resource was used to label the structures to be quantified (collagen fibers). Thus, the collagen and the portal space areas were measured in square micrometers. The collagen area was divided by the area of the region outlined in the portal space, and the value obtained was expressed as the percentage of collagen (ie, fraction of area). In addition, the number of biliary structures was divided by portal space area, obtaining biliary duct density (no. of ducts per square micrometer).

The portal spaces to be evaluated were randomly selected. Portal spaces with area greater than 70,000 μm^2 were excluded. Subsequently, the procedures were repeated so

that the quantification of collagen in the portal spaces of each fragment could be measured [12]. Ten fields per slide were measured for each animal at each phase of the experiment. All measurements were stored in a specific computer program file for subsequent statistical analyses.

1.4. Molecular analysis

1.4.1. Total RNA isolation and reverse transcription

Total RNA was isolated from all liver samples with TRIZOL reagent (Invitrogen, Carlsbad, CA). Approximately 100.0 mg of tissue was fragmented (Mikro Dismembrator U; Sartorius AG, Goettingen, Germany) after the addition of liquid nitrogen and homogenization in 1 mL of TRIZOL reagent. RNA was then isolated with standard procedures.

Total RNA was quantified by spectrophotometry via a Biophotometer (Eppendorf AG, Hamburg, Germany) at an absorbance of 260 nm, and the purity was assessed by determining the 260/280 nm ratio. This ratio ranged from 1.8 to 2.0 for all samples.

The integrity of the isolated RNA sample was determined by denaturing agarose gel electrophoresis through the visualization of the 18S and 28S ribosomal RNA bands after ethidium bromide staining.

Complementary DNA (cDNA) was prepared from the 2.0 μg of total RNA by reverse transcription using 200.0 U of SuperScript III RNase H-RT (Invitrogen) and oligo(dT)s as primers. The resulting cDNA solution was stored at −20°C.

1.4.2. Polymerase chain reaction and semiquantitative analysis of PCR products

The specific primers used in our studies for α-SMA, desmin, and TGF-β1 were designed from the rat messenger RNA (mRNA) sequences obtained from GenBank database (accession no. NM 031004, NM 022531, and NM 021578, respectively). In all experiments, cyclophilin was used as a housekeeping control gene. The primer sequences for the genes were as follows: α-SMA, 5′ GTT CGC GCT CTC CGA AGT TC 3′ (forward) and 5′ CTG TTG TAC AAA GCG AGC ACC G 3′ (reverse); desmin, 5′ CCA ACT GAG AGA AGA AGC AGA G 3′ (forward) and 5′ CTT ATT GGC TCG CTG AGT CAA G 3′ (reverse); TGF-β1, 5′ CCA AAC TAA GGC TCG CCA GTC 3′ (forward) and 5′ CTA CGT GTT GCT CCA CAG TTG 3′ (reverse); and cyclophilin, 5′ GGG AAG GTG AAA GAA GGC AT 3′ (forward) and 5′ GAG AGC AGA GAT TAC AGG GT 3′ (reverse). Polymerase chain reaction was performed according to techniques previously used in our laboratory and described in other similar experiments [13,14]. Each PCR reaction was repeated 3 times to assure data consistency.

1.4.3. Data analysis

Gel images were captured with a Kodak Gel Logic 100 Imaging System (Kodak, Rochester, NY). The density of the PCR bands was determined by Kodak Molecular Imaging Software. The densities were expressed as the ratio of the band density of the target gene divided by that of the housekeeping gene cyclophilin.

1.4.4. Real-time PCR

Real-time PCR was performed only for the α-SMA gene. The primers used to amplify this gene were the same used in the reaction of semiquantitative RT-PCR, but we had to use hypoxanthine phosphoribosyl-transferase as the normalization control gene because in real-time PCR, the reactions run together, and the annealing temperatures should be the same for both reactions. The primer sequences for hypoxanthine phosphoribosyl-transferase were as follows: 5′ CTG ATG GAC TGA TTA TGG ACA GGA 3′ (forward) and 5′ GCA GGT CAG CAA AGA ACT TAT AGC C 3′ (reverse).

Quantitative real-time PCR was performed in a 15.0-μL reaction mix using 7.5-μL Platinum SYBER Green qPCR SuperMix-UDG (Invitrogen), 0.3-μL gene-specific forward and reverse primers (10 μM), 1.0-μL cDNA, and 5.9-μL nuclease-free water.

The cycling conditions were as follows: initial template denaturation at 95°C for 1 minute, followed by 40 cycles of denaturation at 95°C for 20 seconds, annealing at 60°C for 30 seconds, and extension at 72°C for 30 seconds.

The reactions were prepared separately for each of the genes but were amplified together in Rotor-Gene RG-3000 (Corbett Research, Australia). The reaction was run in triplicate. Blank controls were included in parallel for each master mix.

Amplification was followed by a melting curve analysis to check PCR product specificity. Data were analyzed using the ΔΔCt method. The expression levels were normalized with a relative quantification, and the value of $2^{-\Delta\Delta Ct}$ was calculated (ΔΔCt means the difference between the expressions of the α-SMA and the housekeeping gene) [15].

1.5. Second phase of experiments

To properly characterize the experimental model and confirm the findings of the experiments, 15 animals were operated on in another time. The animals were operated on according to the technique previously described, and they were divided in 3 groups of 5 animals per group according to the day of killing: after 1 day, 1 week, and 4 weeks. At the moment of the killing, the ligated and nonligated liver lobes were collected for histologic analyses, and blood samples were collected for biochemical determinations (aspartate aminotransferase [AST], alanine aminotransferase [ALT], γ-glutamyltransferase [GGT], direct bilirubin, and total bilirubin).

1.6. Statistical analysis

Student *t* test was used to compare the weights of the animals. The histomorphometrical and semiquantitative RT-

PCR data were expressed graphically with mean or median values. Because they had a parametric distribution, statistical comparisons were performed by analysis of variance with post hoc Tukey test. Gene expression data obtained by real-time PCR were analyzed by Kruskal-Wallis test with post hoc Tukey test. The hypothesis of sample equality was rejected for $P < .05$. The results of biochemical determinations performed in the second phase of the experiments were compared by analysis of variance and post hoc Tukey test.

2. Results

2.1. Weight and survival rate of animals

All the animals had a good postoperative course without any sign of obstructive jaundice. However, in comparison with controls, they ate less, and the weight gain was decreased (Table 1). The mean survival rate considering all experimental groups was 83%. Deaths were mainly related to bleeding from the liver surface when the clip was inserted.

2.2. Histologic analysis

2.2.1. Hematoxylin-eosin staining

An evident ductular proliferation was observed in portal spaces 1 week after the procedure. The intensity of this alteration decreased during the next 2 weeks and was noticed again after week 4. Such findings were similar in both BO and NBO parenchymas. Finally, despite the ligation of bile duct, in ligated lobes, there were no findings indicating cholangitis, and in the nonligated lobes, no cholestatic changes were observed.

Table 1 Weights of the animals (mean ± SD)

Group	Initial weight	Final weight
1 wk	67.85 ± 3.76	125.28 ± 5.21 *, †
Control	64.83 ± 4.40	142.00 ± 2.60
2 wk	67.28 ± 4.15	176.20 ± 13.33 *, ‡
Control	69.40 ± 3.36	206.40 ± 3.43
3 wk	61.57 ± 1.71	207.83 ± 4.66 *, §
Control	63.60 ± 2.30	228.20 ± 2.38
4 wk	72.57 ± 4.89	236.40 ± 18.60 *, ‖
Control	70.80 ± 5.16	317.66 ± 42.38
8 wk	75.00 ± 2.88	258.16 ± 20.10
Control	74.80 ± 2.58	248.80 ± 9.57

Note that, at the end of the experiment, there was a significant reduction of the weights until week 4. At week 8, no difference was observed.

* Significant in comparison with control.

† $P = .009$.

‡ $P = .009$.

§ $P = .009$.

‖ $P = .01$.

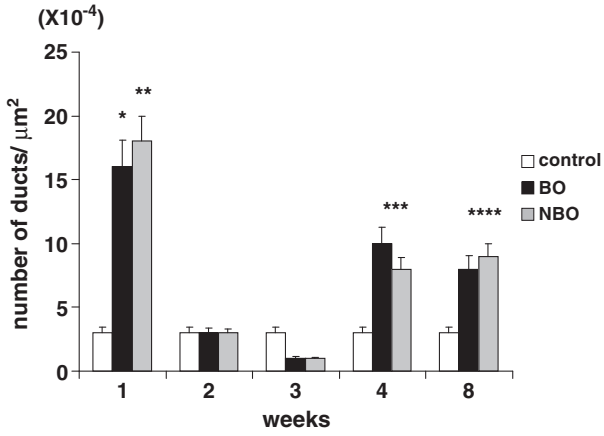

Fig. 2 Values of bile ducts density in each group of animals (mean ± SEM; *$P = .017$, **$P = .009$, ***$P = .03$, ****$P = .027$ compared with the control group).

2.2.2. Quantification of the ductular proliferation and the portal fibrosis by picrosirius staining

The evolution of biliary duct density during the study period is shown in Fig. 2.

Bile ducts' density in both BO and NBO parenchymas was significantly higher than that in controls 1 week after duct ligation ($P = .017$ and $P = .009$, respectively). It decreased close to the control level after 2 and 3 weeks. After 4 weeks, it increased in BO and NBO parenchymas over control ($P = .03$). After 8 weeks, ductular density in BO and NBO parenchymas was significantly higher than in control group ($P = .027$). No differences were verified between BO and NBO parenchymas in all phases of the study.

The evolution of collagen area in portal spaces in BO, NBO, and controls is shown in Fig. 3.

Portal space collagen area increased after 2 weeks in both BO and NBO lobes ($P = .048$ and $P = .031$, respectively, relative to control). After 3 weeks, collagen deposition in BO

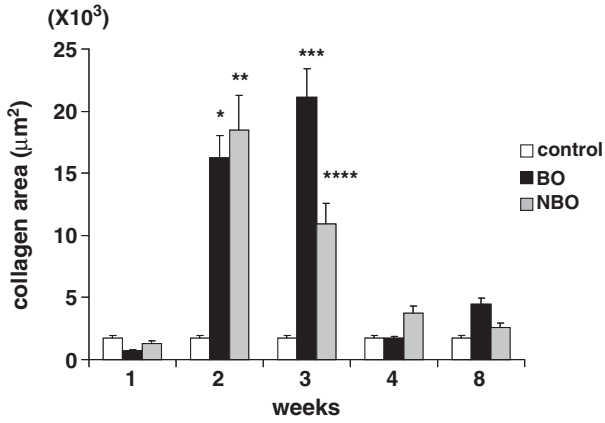

Fig. 3 Collagen area in portal spaces in each group of animals (mean ± SEM; *$P = .048$, **$P = .031$, ***$P = .002$, ****$P = .047$ compared with the control group).

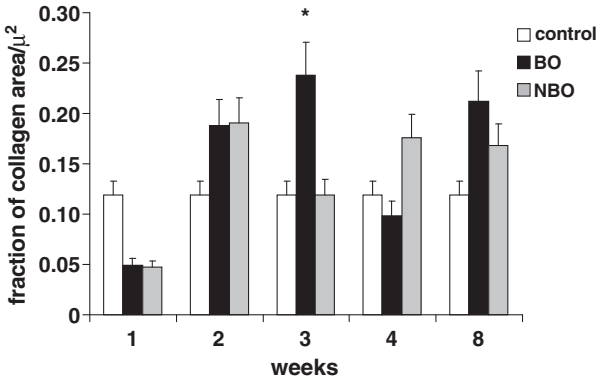

Fig. 4 Fraction of collagen area in portal spaces in each group of animals (mean ± SEM; *P = .035 compared with the control group).

was even higher (P = .002), and thereafter, it diminished. In NBO, collagen area started decreasing after 2 weeks.

The evolution of the fraction of collagen area in the portal space area during the study is shown in Fig. 4. The statistical analysis revealed a significant increase in this parameter in BO parenchyma compared with controls 3 weeks after the operation (P = .0035).

2.3. Molecular analysis

2.3.1. Semiquantitative analysis of PCR products and real-time PCR

The gene expression of desmin and TGF-β1 genes in controls, BO, and NBO hepatic lobes 1 and 8 weeks after the surgery is presented in Fig. 5. Values are expressed by median of percentiles of the relative densities of the bands after the products were run on agarose gels and photographed. No difference among the groups was detected. The semiquantification and quantification of α-SMA expression in controls, BO, and NBO 1 and 8 weeks after the surgery are shown in Fig. 6. The semiquantification by RT-PCR demonstrated that the gene expression was increased in BO hepatic lobes 1 week after the surgery (P = .004). After 8 weeks, the expression of this gene was increased in both BO and NBO lobes (P = .008 and P = .029, respectively). The quantitative method of real-time PCR confirmed that α-SMA gene expression was increased in both BO and NBO hepatic lobes, and this phenomenon was more intense in BO hepatic lobes. Similar findings were observed 1 and 8 weeks after selective biliary ligation (P = .002, P = .005, P = .0001, and P = .002, respectively,

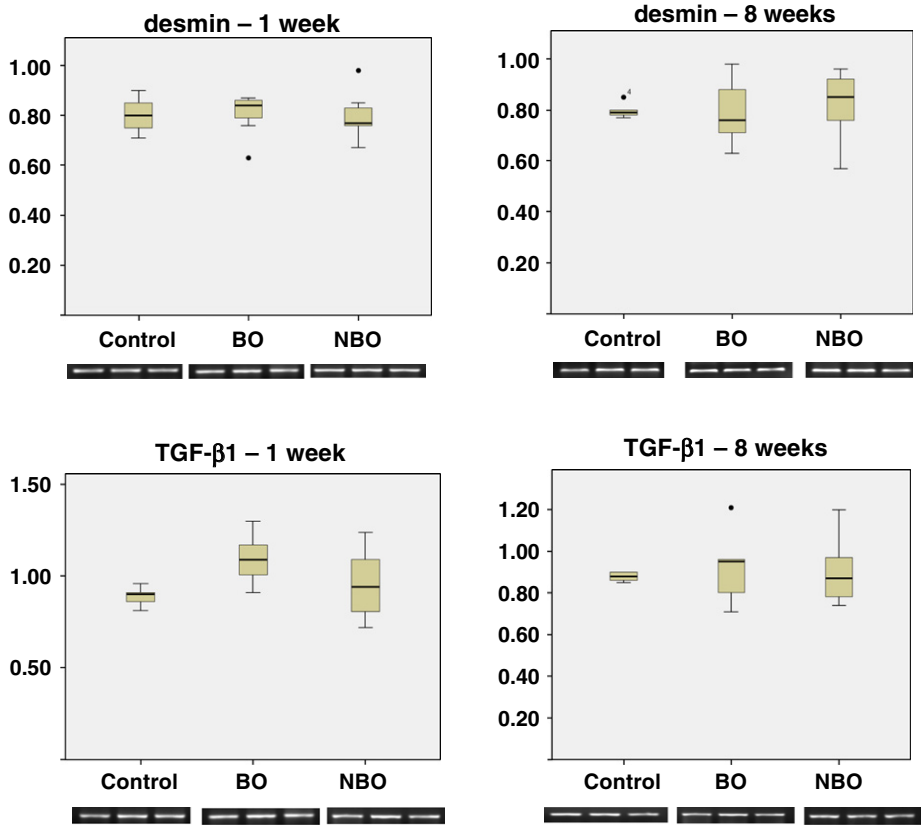

Fig. 5 Reverse transciptase–PCR–relative band density of each group (median) for the desmin and TGF-β1 genes (1 and 8 weeks after the surgery) and the mRNA expression levels represented by the bands (below, repeated 3 times to assure data consistency). No difference among the groups was detected. The numbers inside the graphics are outliers.

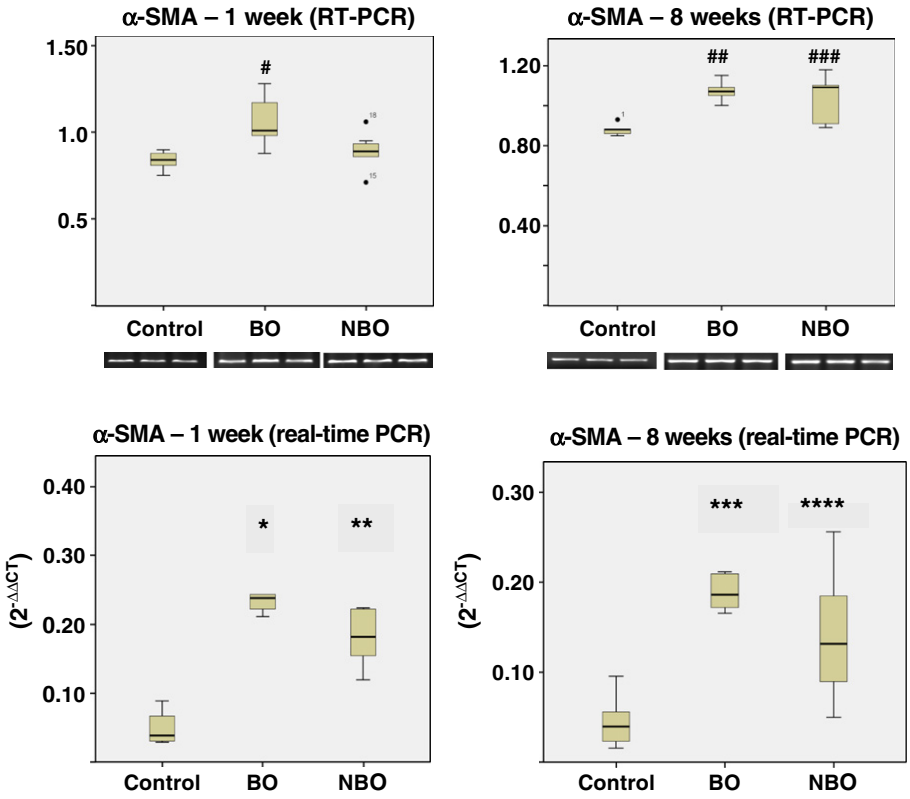

Fig. 6 Reverse transciptase–PCR–relative band density of each group (median) for α-SMA gene (1 and 8 weeks after the surgery) and the expression levels represented by the bands, repeated 3 times ($^{\#}P = .004$, $^{\#\#}P = .008$ and $^{\#\#\#}P = .029$, compared with the control group). Below are the results of real-time PCR ($^{*}P = .002$, $^{**}P = .005$, $^{***}P = .0001$, $^{****}P = .002$ compared with the control group; no difference between BO and NBO was detected). The numbers inside the graphics are outliers.

compared with control group). In addition, no statistical difference between BO and NBO was detected.

2.4. Second phase of experiments

The results obtained in the second phase of experiments confirmed the findings encountered in the experimental groups. The histologic alterations characterizing BO in both BO and NBO lobes were detected early in the first day after the operation. These findings persisted until the fourth week after the bile ducts ligation (Fig. 7). The results of biochemical determinations are summarized in Table 2. In the first day after the selective ligation of biliary ducts, a significant increase in the seric levels of AST, ALT, GGT, and bilirubins was detected. After 1 and 4 weeks, the levels of enzymes and bilirubins returned to normal values.

3. Discussion

The studies on experimental cholestasis obtained from bile duct ligation experimental models have been mostly performed in adult animals. Experiments with newborn and young animals face intraoperative technical difficulties because of the dimensions of the anatomical structures, special anesthetic procedures, the need for microsurgical instruments, and problems in keeping the animals alive for the duration of the experiment [16]. All of these factors contribute to making the use of young animals in experiments more difficult and, consequently, more sporadic.

In previous experiments using rats subjected to BDL, significant differences were observed between the responses of animals of different ages regarding the ductule proliferation [8]. In addition, the increase in desmin expression was more intense and precocious in newborn than in adult rats [17]. Similar results were obtained by Medeiros et al [18] when studying the histologic differences secondary to common bile duct obstruction in adult and young rats with a mean weight of 20 g during periods of 4 to 40 days after BDL. The authors observed a slower inflammatory response in young animals when compared with adults and a faster evolution to regenerative nodule formation and cirrhosis in young animals. Omori et al [19], using a model of BO in young rats and comparing them with adult rats, studied the liver tissue expression of α-fetoprotein. They found that ductule proliferation and fibrogenesis were more intense in the young rat when compared with the adults. They also observed differences

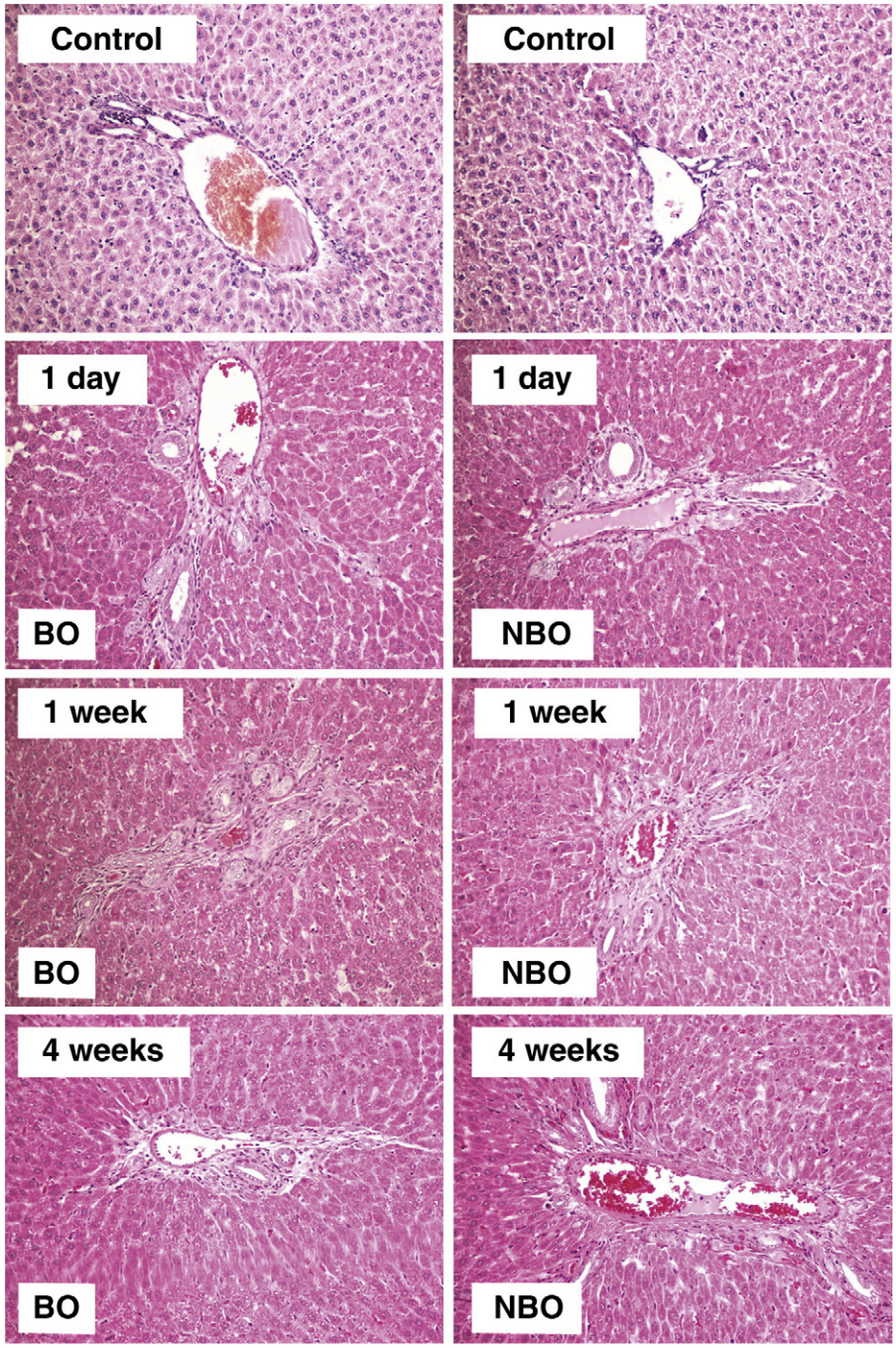

Fig. 7 Histologic alterations in BO and NBO lobes. Note that the portal spaces are expanded because of intense ductular proliferation in both BO and NBO lobes. These alterations are observed early in the first day after the ligation of bile duct and persisted until the fourth week (original magnification ×200).

in the tissue expression of α-fetoprotein during the developmental process, and it was absent in the adult animals. Zimmermann et al [20], studying the BDL model in rats for a period of 4 weeks, studied 4-, 7-, 14-, and 22-week-old rats and compared them with adult animals. They found that the development of cirrhosis secondary to BO in rats was age dependent during the developmental period and that the adult animals presented more fibrogenesis when compared with the young animals.

Selective BO is difficult to achieve in rats. Besides the technical difficulties related to the size of biliary lobar ducts and the proximity to arterial branches, the existence of interlobar accessory bile channels and fast bile duct collateral formation is responsible for the rapid recovery from obstructive cholestasis in rats, as demonstrated by the microcholangiography and magnetic resonance studies by Ni et al [21]. In fact, histologic alterations after selective BO could only be obtained in our animal model after the

Table 2 Biochemical determinations of animal groups (mean ± SD)

Group	AST (IU/L)	ALT (IU/L)	GGT (IU/L)	DB (mg/dL)	TB (mg/dL)
Control	210.60 ± 30.47	60.20 ± 8.76	5.20 ± 0.45	0.11 ± 0.03	0.18 ± 0.05
1 d	1607.40 ± 525.0 *	383.60 ± 64.5 *	8.60 ± 2.41 †	0.23 ± 0.05 *	0.40 ± 0.07 *
1 wk	241.01 ± 50.50	70.75 ± 15.39	7.75 ± 0.96	0.05 ± 0.01	0.19 ± 0.06
4 wk	200.75 ± 53.12	88.01 ± 17.34	3.00 ± 0.82	0.02 ± 0.02 ‡	0.17 ± 0.03

Note the elevated levels of seric enzymes and bilirubins 1 day after the selective ligation. All these parameters returned to normal values after 1 and 4 weeks. DB indicates direct bilirubin; TB, total bilirubin.

* $P < .001$ relative to control.

† $P = .016$ relative to control.

‡ $P = .008$ relative to control.

introduction of the second step of the surgery, consisting of clamping the parenchyma connection between the right and median liver lobes.

Sequential evaluation of biliary duct density after selective BO revealed an intense ductular proliferation 1 week after the procedure, followed by a decrease in ductular density during the next 2 weeks. These findings are similar to those observed in the model of common bile duct ligation [8] and may be explained by bile duct collateral neoformation in the hilum area and by collagen deposition and expansion of the portal area (which increases the denominator of the duct density ratio). The subsequent increase in biliary duct density after the fourth week suggests the maintenance of any stimulus to biliary proliferation. Interestingly, there was similar ductular evolution in BO and NBO, leading to the hypothesis of the existence of paracrine and endocrine stimulatory factors to biliary proliferation during regional cholestasis.

Gastrointestinal hormones, biliary acids, angiogenic factors, neurotransmistters, and steroid hormones influence the proliferative response of cholangiocytes to cholestasis [22]. It is possible that one or some of them act in the adjacent noncholestatic parenchyma, leading to a similar proliferative response.

Analysis of collagen deposition in the portal space revealed intense fibrogenesis during the second and third weeks followed by a decrease in collagen quantity after the fourth week. Similar to the ductular reaction, the observed collagen portal space evolutions of BO and NBO were similar.

It may be supposed that biliary proliferation during the first week was responsible for portal fibrogenesis during the next 2 weeks. The formation of bile ducts collaterals could lead to a diminution in the ductular reaction after the second week and, as a consequence, a decrease in collagen deposition during the fourth and eighth weeks. In fact, proliferating colangiocytes secrete profibrogenic factors, leading to the activation of fibroblasts and hepatic stellate cells [23,24]. Moreover, the cholangiocytes may acquire phenotypic characteristics of mesenchymal cells, a process called *ephitelial-mesenchymal transition* [25,26].

There have been few molecular studies in animal models of cholestasis. To study the effects of cholestasis in liver ischemic injury and postischemic inflammation, Georgiev et al [27] performed a common BDL (BO with hyperbilirubinemia) and selective ligation of the left hepatic duct (BO without hyperbilirubinemia) in mice before 1 hour of hepatic ischemia and reperfusion. Cholestatic mice showed considerable protection from ischemic liver injury, as determined by transaminase release, histologic liver injury, and neutrophil infiltration. In cholestatic mice, reduced injury correlated with a failure to activate mRNA synthesis of nuclear factor κB and tumor necrosis factor α, 2 key mediators of postischemic liver inflammation. After selective bile duct ligation, both the ligated and nonligated lobes showed blocked activation of nuclear factor κB as well as reduced induction of tumor necrosis factor α mRNA synthesis and neutrophil infiltration. Therefore, similar to our findings, cholestatic liver parenchyma protected the adjacent noncholestatic lobe against ischemic injury.

We observed that α-SMA gene expression increased in BO liver parenchyma 1 week after selective biliary ligation. After 8 weeks, its expression was higher in NBO as well. The α-SMA is expressed by hepatic myofibroblasts, which constitute a heterogeneous population of highly proliferative, profibrogenic, proinflammatory, proangiogenic, and contractile cells that sustain liver fibrogenesis and then fibrotic progression of chronic liver diseases of different etiologies to the common advanced stage of cirrhosis. These cells originated from a process of activation and transdifferentiation that involves either hepatic stellate cells or fibroblasts of portal areas [28]. Based on our results, we may infer that selective BO led to an increase in myofibroblast population in both cholestatic and adjacent liver parenchymas, and this was associated with a collagen deposition and portal fibrosis.

Therefore, we conclude that the ligation of a duct responsible for biliary drainage of a liver lobe led to alterations in the parenchyma and in the adjacent nonobstructed parenchyma by paracrine and/or endocrine means. This was supported by the histologic findings and the increased expression of α-SMA, a protein related to hepatic fibrogenesis and expressed by the stellate cells. These results may help elucidate the pathophysiologic mechanisms of biliary atresia and apply directly to intrahepatic biliary stenosis, mainly after liver transplantation. Finally, future experiments including the study of biochemical indicators of liver injury and using other growing animals such as the

newborn suckling rats will be needed to confirm the results of the present investigation.

References

[1] Ramm GA, Nair VG, Bridle KR, et al. Contribution of hepatic parenchymal and nonparenchymal cells to hepatic fibrogenesis in biliary atresia. Am J Pathol 1998;153:527-35.

[2] Li MK, Crawford JM. The pathology of cholestasis. Semin Liver Dis 2004;24:21-42.

[3] Moreira AM, Carnevale FC, Tannuri U. Long-term results of percutaneous bilioenteric anastomotic stricture treatment in liver-transplanted children. Cardiovasc Intervent Radiol 2010;33:90-6.

[4] Armendariz-Borunda J, Simkevich CP, Roy N, et al. Activation of Ito cells involves regulation of AP-1 binding proteins and induction of type I collagen gene expression. Biochem J 1994;304:817-24.

[5] Rodriguez-Garay EA. Cholestasis: human disease and experimental animal models. Ann Hepatol 2003;2:150-8.

[6] Friedman SL, Yamasaki G, Wong L. Modulation of transforming growth factor-β receptors of rat lipocytes during the hepatic wound healing response: enhanced binding and reduced gene expression accompany cellular activation in culture and in vivo. J Biol Chem 1994;269:10551-8.

[7] Rippe RA, Almounajed G, Brenner DA. Sp-1 binding activity increases in activated Ito cells. Hepatology 1995;251:241-51.

[8] Gibelli NE, Tannuri U, Mello ES, et al. Bile duct ligation in neonatal rats: is it a valid experimental model for biliary atresia studies? Pediatr Transplant 2009;13:81-5.

[9] Kountouras J, Billing BH, Scheuer PJ. Prolonged bile duct obstruction: a new experimental model for cirrhosis in the rat. Br J Exp Pathol 1984;65:305-11.

[10] Wang P, Gong G, Wei Z, et al. Ethyl pyruvate prevents intestinal inflammatory response and oxidative stress in a rat model of extrahepatic cholestasis. J Surg Res 2010;160:228-35.

[11] COBEA (Colégio Brasileiro de Experimentação Animal); Ethic Commission for animal experimentation. Available in http://www.cobea.org.br.

[12] Masseroli M, Caballero T, O'Valle F, et al. Automatic quantification of liver fibrosis: design and validation of a new image analysis method: Comparison with semi-quantitative indexes of fibrosis. J Hepatol 2000;32:453-64.

[13] Coelho MC, Tannuri U, Tannuri AC, et al. Expression of interleukin 6 and apoptosis-related genes in suckling and weaning rat models of hepatectomy and liver regeneration. J Pediatr Surg 2007;42:613-9.

[14] Tannuri U, Tannuri AC, Coelho MC, et al. Effect of the immunosuppressants on hepatocyte cells proliferation and apoptosis during liver regeneration after hepatectomy—molecular studies. Pediatr Transplant 2008;12:73-9.

[15] Pfaffl MW. A new mathematical model for relative quantification in real-time RT-PCR. Nucleic Acids Res 2001;29:2002-7.

[16] Tannuri AC, Tannuri U, Coelho MC, et al. Experimental models of hepatectomy and liver regeneration using newborn and weaning rats. Clinics (Sao Paulo) 2007;62:757-62.

[17] Gibelli NE, Tannuri U, Mello ES. Immunohistochemical studies of stellate cells in experimental cholestasis in newborn and adult rats. Clinics (Sao Paulo) 2008;63:689-94.

[18] Medeiros MV, Freitas LA, Andrade ZA. Differences in hepatic pathology resulting from bile duct obstruction in young and old rats. Braz J Med Biol Res 1988;21:75-83.

[19] Omori M, Evarts RP, Omori N, et al. Expression of alpha-fetoprotein and stem cell factor/c-kit system in bile duct ligated young rats. Hepatology 1997;25:1115-22.

[20] Zimmermann H, Blaser H, Zimmermann A, et al. Effect of development on the functional and histological changes induced by bile-duct ligation in the rat. J Hepatol 1994;20:231-9.

[21] Ni Y, Lukito G, Marchal G, et al. Potential role of bile duct collaterals in the recovery of the biliary obstruction: experimental study in rats using microcholangiography, histology, serology and magnetic resonance imaging. Hepatology 1994;20:1557-66.

[22] Glaser SS, Gaudio E, Miller T, et al. Cholangiocyte proliferation and liver fibrosis. Expert Rev Mol Med 2009;11:e7.

[23] Sedlaczek N, Jia JD, Bauer M, et al. Proliferating bile duct epithelial cells are a major source of connective tissue growth factor in rat biliary fibrosis. Am J Pathol 2001;158:1239-44.

[24] Milani S, Herbst H, Schuppan D, et al. Procollagen expression by nonparenchymal rat liver cells in experimental biliary fibrosis. Gastroenterology 1990;98:175-84.

[25] Sicklick JK, Choi SS, Bustamante M, et al. Evidence for epithelial-mesenchymal transitions in adult liver cells. Am J Physiol Gastrointest Liver Physiol 2006;291:G575-83.

[26] Omenetti A, Yang L, Li YX, et al. Hedgehog-mediated mesenchymal-epithelial interactions modulate hepatic response to bile duct ligation. Lab Invest 2007;87:499-514.

[27] Georgiev P, Navarini AA, Eloranta JJ, et al. Cholestasis protects the liver from ischaemic injury and post-ischaemic inflammation in the mouse. Gut 2007;56:121-8.

[28] Novo E, di Bonzo LV, Cannito S, et al. Hepatic myofibroblasts: a heterogeneous population of multifunctional cells in liver fibrogenesis. Int J Biochem Cell Biol 2009;41:2089-93.